Published in final edited form as:
Exp Gerontol. 2009 April ; 44(4): 261–273. doi:10.1016/j.exger.2008.09.013.

Role of Ca^{2+}, Membrane Excitability, and Ca^{2+} Stores in Failing Muscle Contraction with Aging

Anthony Michael Payne[2,#], **Ramón Jimenez-Moreno**[1], **Zhong-Ming Wang**[1], **María Laura Messi**[1], and **Osvaldo Delbono**[1,2,3,*]

[1]Department of Internal Medicine, Section on Gerontology and Geriatric Medicine, Wake Forest University School of Medicine, Winston-Salem, NC 27157

[2]Department of Physiology and Pharmacology, Wake Forest University School of Medicine, Winston-Salem, NC 27157

[3]Neuroscience Program, Wake Forest University School of Medicine, Winston-Salem, NC 27157

Abstract

Excitation-contraction (EC) coupling in a population of skeletal muscle fibers of aged mice becomes dependent on the presence of external Ca^{2+} ions (Payne et al., 2004b). However, the mechanism(s) underlying this process remain unknown. In this work, we examined the role of 1) extracellular Ca^{2+}; 2) voltage-induced influx of external Ca^{2+} ions; 3) sarcoplasmic reticulum (SR) Ca^{2+} depletion during repeated contractions; 4) store-operated Ca^{2+} entry (SOCE); 5) SR ultrastructure; 6) SR subdomain localization of the ryanodine receptor; and 7) sarcolemmal excitability in muscle force decline with aging. These experiments show that external Ca^{2+}, but not Ca^{2+} influx, is needed to maintain force upon repetitive fiber electrical stimulation. Decline in fiber force is associated with depressed SR Ca^{2+} release. SR Ca^{2+} depletion, SOCE, and the putative segregated Ca^{2+} release store do not play a significant role in external Ca^{2+}-dependent contraction. More importantly, a significant number of action potentials fail in senescent mouse muscle fibers subjected to a stimulation frequency. These results indicate that failure to generate action potentials accounts for decreased intracellular Ca^{2+} mobilization and tetanic force in aging muscle exposed to a Ca^{2+}-free medium.

Keywords

Aging; skeletal muscle; calcium; sarcoplasmic reticulum; dihydropyridine receptor; ryanodine receptor

Introduction

It is generally accepted that mammalian skeletal muscle excitation-contraction coupling occurs through a mechanical interaction between the L-type voltage sensitive Ca^{2+} channel of the sarcolemma – dihydropyridine receptor (DHPR) – and the Ca^{2+} release channel of the sarcoplasmic reticulum (SR) – ryanodine receptor type 1 (RyR1) – as opposed to an inward Ca^{2+} current through the DHPR (Armstrong et al., 1972; Dulhunty and Gage, 1988; González-Serratos et al., 1982; Rios and Brum, 1987; Tanabe et al., 1990b; Tanabe et al.,

* **Corresponding Author:** Osvaldo Delbono, Department of Internal Medicine, Section on Gerontology and Geriatric Medicine, Wake Forest University School of Medicine, 1 Medical Center Boulevard, Winston-Salem, NC 27157, Phone: (336) 716-9802. Fax: (336) 716-2273, odelbono@wfubmc.edu.
# Current address: Department of Applied Physiology and Kinesiology, College of Health and Human Performance, University of Florida, Gainesville, Florida.

1990a). Our laboratory has studied how aging leads to alterations in EC coupling that contribute to age-related specific force decline, termed “EC uncoupling” (Delbono et al., 1995; González et al., 2003; Renganathan et al., 1997; Wang et al., 2000). We also reported that EC coupling in aged mouse skeletal muscle becomes dependent on the presence of external Ca^{2+} ions, in opposition to what is accepted for young adult non-injured skeletal muscle (Payne et al., 2004b). Aging muscle experiences a slow denervation process (Einsiedel and Luff, 1992; Kadhiresan et al., 1996; Larsson and Ansved, 1995), and our lab has reported on the importance of denervation in age-related changes in EC coupling (Delbono, 2003; Payne and Delbono, 2004). Specifically, we recently reported that preventing denervation by targeting the potent growth factor IGF-1 to spinal cord motor neurons prevent age-related decreases in muscle fiber specific force (Payne et al., 2006), providing further evidence for denervation as an underlying cause in age-related alterations in EC coupling. In investigating potential underlying causes for dependence on external Ca^{2+} in aged mouse skeletal muscle to sustain tetanic force, we have now also reported that targeting IGF-1 to spinal cord motor neurons prevents external Ca^{2+}-dependent EC coupling (Payne et al., 2007).

The specific molecular mechanism(s) of external Ca^{2+}-dependent EC coupling and whether this phenomenon leads to functional deficits in aged muscle are yet unknown. To better understand external Ca^{2+}-dependent EC coupling in aged mammalian skeletal muscle, we performed experiments to explore the following possibilities: 1) that the presence of external Ca^{2+} is needed to sustain contraction force; 2) that aged muscle is dependent on the voltage-induced influx of external Ca^{2+} ions; 3) that aged muscle SR becomes depleted of Ca^{2+} during repeated contractions in Ca^{2+}-free medium; 4) that store-operated Ca^{2+} entry (SOCE) is necessary to maintain SR Ca^{2+} stores in aged muscle during repeated contractions; 5) that a segregated SR Ca^{2+} store (Weisleder et al., 2006) accounts for the deficit in SR Ca^{2+} release in Ca^{2+}-free medium; and 6) that the generation of action potentials fails in response to high frequency stimulation.

Materials and Methods

Animals

Young (3–6 mo) and old FVB (22–24 mo; our colony), DBA (21 mo; NIA) or CB6F1 (33 mo; NIA) mice were housed at Wake Forest University School of Medicine and all procedures were approved by the Animal Care and Use Committee. Differences in the age of these mouse strains relates to their relative life spans. FVB and DBA strains have been successfully used in the study of aging muscle in previous work from our lab (González et al., 2000; González et al., 2003; Renganathan et al., 1998) and the CB6F1 strain has been used by other investigators (Miller et al., 1997). The availability of the oldest animals determined the inclusion of three mouse strains in the present work.

Single Intact Muscle Fiber Contraction

At time of sacrifice, flexor digitorum brevis (FDB) muscles were carefully dissected and pinned into a Petri dish lined with Sylgard (Dow Corning, Auburn, MI) in a Ca^{2+}-containing physiological solution (see below). All contraction experiments were carried out at room temperature (21–22°C). Single intact fiber dissection followed procedures previously published (González et al., 2000; Lannergren and Westerblad, 1987). Following dissection, tendons of single intact fibers were placed in custom-made micro-clips, and these clips were connected to a force transducer and a micropositioner for length control. Fibers were adjusted to optimum length (L_O) by using single twitches, elicited by 0.5-ms square wave pulses at 10 V. Once at L_O, fibers were stimulated with 350-ms trains of pulses, using frequencies varying from 50 to 100 Hz. The stimulation frequency that elicited maximum

force was used for the remainder of the experiment. Preliminary data (not shown) showed that DBA and CB6F1 mice exhibit a similar proportion of fibers which force decline in Ca^{2+}-free solution (Affected) and those which do not (Unaffected) as reported previously for FVB mice (Payne et al., 2004b). Approximately equal number of fibers from the three mouse strains was included within a given experiment.

Cd^{2+} experiment—Fibers underwent two similar prolonged contractile sequences (0Ca trial and Cd trial). Tetanic contractions were elicited every 20 seconds for 25 min (75 total contractions) in modified Ringer's solutions (see below). During the 0Ca trial, standard Ringer's solution was replaced with a Ca^{2+}-free Ringer from min 5–15 (contractions 16–45). After 15 min of recovery the Cd trial was performed by replacing standard Ringer solution with a Cd^{2+}-containing Ringer solution (0.5 $CdCl_2$ added) from min 5–15. The change in base solution versus previously published methods is due to the immediate precipitation of Cd^{2+} upon introduction to a solution with PO_4^-. The longer interval between tetanic contractions versus previously published methods was to prevent fatigue development in this solution. Force decline during min 5–15 of the 0Ca trial was compared to force decline during the same time period of the Cd trial.

4-CmC contracture experiment—Intact fibers underwent one contraction sequence (one contraction every 10 sec for 15 min; 90 total contractions). Ca^{2+}-free physiological solution was replaced by Ca^{2+}-free physiological solution (see below) from min 5–15. Immediately upon the ending of repeated tetanic contractions, solution was switched again to a Ca^{2+}-free physiological solution containing 1 mM 4-chloro-*m*-cresol (4-CmC) in DMSO (1% DMSO final concentration) to elicit a contracture.

2-APB experiments—Fibers underwent two contractile sequences. The first was identical to the 0Ca trial mentioned above, followed by up to 15 min recovery, to indicate which fibres exhibited force decline in Ca^{2+}-free solution (see below). The second sequence followed one of two approaches. In the first approach, physiological solution was perfused from min 0–5, Ca^{2+}-free physiological solution was perfused from min 5–15, Ca^{2+}-free solution with 20 μM 2-aminoethoxydiphenyl borate (2-APB) was perfused from min 15–20, Ca^{2+}-containing physiological solution with 20 μM 2-APB was perfused for 10 min, followed by standard physiological solution for the final 10 min. 2-APB is a store-operated Ca^{2+} entry (SOCE) blocker (Bootman et al., 2002; Gonzalez Narvaez and Castillo, 2007; Pan et al., 2002). The second approach was used for fibers which exhibited dramatic force decline (>95%) in Ca^{2+}-free solution. In this approach, 20 μM 2-APB was introduced simultaneously with physiological solution for 10 min, upon loss of fiber contractile activity, followed by standard physiological solution for the remainder of the experimental procedure. As a control, some fibers underwent a standard 150-contraction protocol, during which 20 μM 2-APB was perfused from min 5–15 (contractions 31–90) to assess the effects of 2-APB itself. Force decline was assessed during the period in Ca^{2+}-free solution, while force recovery was assessed during the period in the standard solution with 20 μM 2-APB.

High-Mg^{2+} experiments—Fibers underwent one of two experimental procedures. In the first, fibers endured two contractile sequences (0Ca trial and high-Mg trial) as above. The 0Ca trial was identical to above. The high-Mg trial was the same protocol with a Ca^{2+}-free solution containing elevated [Mg^{2+}] (see below) perfused from min 5–15. Force decline during min 5–15 of the 0Ca trial was compared to force decline during the same time period of the high-Mg trial. In the second experimental procedure, fibers were placed in the experimental chamber and incubated in 5 μM Fluo-4 AM for 45 min. After a 15 min washout, modified versions of the aforementioned 0Ca and high-Mg trials were performed, as previously published (Payne et al., 2004b). In these trials, baseline measurements were

made, followed by 10 min perfusion with Ca^{2+}-free solution, then 10 min of physiological solution perfusion, eliciting one tetanic contraction every 2 min while intracellular fluorescence was measured simultaneously. The modified 0Ca and high-Mg trials followed the same procedure.

Immunostaining for RyR1

EDL muscles were dissected and pinned in Petri dishes lined with Sylgard in Ringer solution (see above). Bundles of fibers were dissected from EDL muscles (4 bundles corresponding to the 4 distal tendons) and pinned to the bottom of embedding molds. The bundles were pinned by one tendon, aligned to a resting length, then stretched 20% (using a dissection scope with ruler), and the final tendon was pinned. The bundles were covered with OCT embedding medium, and quickly frozen by immersion in isopentane cooled with dry ice to −40°C. Longitudinal sections (30 μm thick) were cut with a cryostat. Sections were placed on a slide in a drop of 3% disodium EDTA (to prevent contracture of muscle fibers), air dried at 37°C, then stored in a refrigerator. For immunofluorescent staining, slides were washed in PBS for 5 min, sections were fixed in 4% paraformaldehyde in PBS for 15 min, followed by four 15-min washes in PBS. Sections were blocked with 5% normal rabbit serum, 0.5% Triton X-100, 0.2% BSA in PBS for 1 hr at room temperature. Sections were incubated for 1 hr in primary antibody (34C; Developmental Studies Hyridoma Bank, University of Iowa, IA, (Airey et al., 1990)) diluted 1:200 in 2% normal rabbit serum, 0.5% Triton X-100, 0.2% BSA in PBS, then washed 3 times in PBS for 5 min each. Finally, sections were incubated in an FITC conjugated rabbit anti-mouse secondary antibody (Jackson ImmunoResearch Laboratories, West Grove, PA) diluted 1:400 in 2% normal rabbit serum, 0.5% Triton X-100, 0.2% BSA in PBS for 1 hr, then washed 4 times in PBS for 5 min each and mounted with fluorescence mounting medium. Confocal *XY* images were obtained on a BioRad Radiance 2100 confocal laser scanning microscope (BioRad, Hercules, CA) attached to a Zeiss Axiovert 100 (Carl Zeiss, Thornwood, NY) using a 100×, 1.3 NA oil immersion FLUAR objective (Zeiss). Fluorescence intensity profiles were analyzed on ImageJ software (NIH).

Transmission Electron Microscopy

Samples were prepared for EM as described (Felder et al., 2002; Saito et al., 1984), with modifications. EDL muscles were fixed in 2.5% glutaraldehyde in 100 mM sodium cacodylate buffer at room temperature (pH 7.4) and stored in sodium cacodylate buffer at 4°C. Two to four fiber samples were cut from different areas of the fixed EDL muscles, washed with sodium cacodylate buffer three times, postfixed in 2% OsO4 in cacodylate buffer for 1–2 hours at room temperature, and stained en bloc with saturated aqueous uranyl acetate (UA) overnight. Fiber samples were then embedded in Spurr resin and thin sectioned (<50 nm). Three to four sections were cut from each fiber sample, and then mounted for further staining. The resulting sections, now on Formvar-coated capper slot grids, were stained again with UA solution and modified Sato's lead solution (0.4% w/v calicined lead citrate, 0.3% lead acetate, 0.3% lead nitrate. 2% sodium citrate 0.72% NaOH) (Takagi et al., 1990) for 30–60 minutes each, at room temperature. Staining time in samples from young mice provided optimal contrast at 30 minutes, revealing triads on either side of each Z line. Staining time was increased to 60 minutes for samples from old mice to produce images of sufficient quality for analysis. Longitudinally sliced muscle fibers were imaged by electron microscopy at 60 keV, 50,000× magnification (Carl Zeiss 10-C, Oberkochen, Germany). Micrographs were scanned and images saved for analysis.

Action potential recording

Action potentials were recorded with the two microelectrodes technique in enzymatically dissociated FDB fibers, using a TEV-200A amplifier (Dagan Co., Minneapolis, MN),

DigiData 1322A, and pClamp10 software (MDS Analytical Technologies, Sunnyvale, CA). The external solution was the same used for the contraction experiments with the addition of 50μM N-benzyl-p-toluene sulphonamide (BTS). The recording and current-injecting electrodes were filled with 3M KCl, respectively. Pipette resistance was 10–20MΩ. Fibers were stimulated with 50, 75, or 100 Hz trains of pulses for 350 ms. Fibers were stimulated in physiological solution, then with 10 trains at a 10-second interval in Ca^{2+}-free solution (see below), then again in physiological solution to allow for recovery.

Solutions

The Ca^{2+}-containing physiological solution consisted of (in mM): 121 NaCl, 5 KCl, 1.8 $CaCl_2$, 0.5 $MgCl_2$, 0.4 NaH_2PO_4, 24 $NaHCO_3$, and 5.5 glucose, while the Ca^{2+}-free solution consisted of 121 NaCl, 5 KCl, 2.3 $MgCl_2$, 0.4 NaH_2PO_4, 24 $NaHCO_3$, and 5.5 glucose. The Ca^{2+}-free/high-Mg^{2+} solution was also Ca^{2+}-free and consisted of 117 NaCl, 5 KCl, 5 $MgCl_2$, 0.4 NaH_2PO_4, 24 $NaHCO_3$, and 5.5 glucose. The three solutions were bubbled continuously with 95/5% O_2/CO_2 to maintain pH 7.4. The standard Ringer's solution contained: 145 NaCl, 5 KCl, 2.5 $CaCl_2$, 1 $MgSO_4$, 10 HEPES, 10 Glucose, while the Ca^{2+}-free Ringer solution: 145 NaCl, 5 KCl, 2.5 $MgCl_2$, 1 $MgSO_4$, 10 HEPES, 10 Glucose. Ringer solution's pH 7.4 was reached with NaOH.

Statistical analysis

All data are presented as means ± s.e.m. Data were analyzed with paired student's t-test, regression analysis, or two-way repeated measures ANOVA, with Tukey's multiple comparisons test applied *post hoc* when appropriate. An alpha value of $P < 0.05$ was considered significant.

Results

Role of Ca^{2+} influx in external Ca^{2+}-dependent contraction in aged mouse muscle fibers

We performed experiments pairing contraction protocols in Ca^{2+}-free solution and in physiological solution with the addition of Cd^{2+} to block Ca^{2+} entry. Addition of 0.5mM Cd^{2+} has been shown to eliminate inward Ca^{2+} current (I_{Ca}) in voltage-clamped muscle fibers while in the presence of 2mM Ca^{2+}(Wang et al., 1999). In these experiments, we again found two populations of muscle fibers from aged mice – those which exhibit force decline in Ca^{2+}-free solution and those which do not (Old Affected and Old Unaffected, respectively) (Payne et al., 2004b). Figure 1A shows the effects of Ca^{2+}-free (left) and Cd^{2+}-containing (right) solutions on fibers from young and aged mice. The fibers from old mice could be separated into two groups exhibiting significantly different behavior in Ca^{2+}-free solution (Figure 1B). Fibers from both the Old Unaffected and Old Affected groups showed no force decline in Cd^{2+}-containing solution (Figure 1B). The presence of external Cd^{2+} had no effect on the force of fibers from young mouse muscle (Figure 1A, B). Figure 1C shows the force traces of a representative fiber from the Old Affected group. The left set of traces indicates the 0Ca trial; the right set of traces indicates the Cd trial. Note the force decline in Ca^{2+}-free solution and recovery in physiological solution containing 1.8mM Ca^{2+}, and no force decline in Cd^{2+}-containing solution.

Role of sarcoplasmic reticulum Ca^{2+} depletion in external Ca^{2+}-dependent contraction in aged mouse muscle fibers

In order to examine the possibility of sarcoplasmic reticulum (SR) Ca^{2+} depletion during repeated contractions in Ca^{2+}-free solutions, we conducted experiments in which fibers were perfused with 1 mM 4-CmC in Ca^{2+}-free solution immediately following a series of tetanic contractions in Ca^{2+}-free solution. Figures 2A and B illustrate the tetanic contractions

during the 0Ca trial (left traces) and a contracture evoked by 4-CmC perfusion (right trace) immediately following cessation of tetanic contractions. Figure 2A shows data from a muscle fiber representative of fibers from the Old Unaffected group, which exhibit no force decline while perfused with Ca^{2+}-free solution. Figure 2B shows the same contraction protocol in a fiber from the Old Affected group, which exhibited significant force decline while perfused with Ca^{2+}-free solution. Even though tetanic force responses declined to below measurable levels, a robust 4-CmC contracture could still be evoked in Ca^{2+}-free solution. In fact, the average contracture force in fibers from this group was virtually identical to baseline tetanic force, whereas the average force at the end of the 0Ca trial was significantly reduced (Figure 2C). All fibers from both groups produced robust 4-CmC contractures following repeated tetanic contractions in Ca^{2+}-free solution.

Role of store-operated Ca^{2+} entry (SOCE) in external Ca^{2+}-dependent contraction in aged mouse muscle fibers

In line with the possible explanation that SR Ca^{2+} depletion in Ca^{2+}-free solution causes the observed force decline in aged muscle fibers is the notion that recovery of contractile force should depend upon SR Ca^{2+} store repletion via Ca^{2+} entry. Therefore, we investigated the role of SOCE in force recovery in those fibers which exhibit force decline in Ca^{2+}-free medium. If SR Ca^{2+} depletion is responsible for force decline in Ca^{2+}-free medium, re-exposure to Ca^{2+} should allow SOCE, SR refilling, and force recovery; whereas, blocking SOCE by addition of the well-characterized SOCE blocker 2-APB (Bootman et al., 2002; Gonzalez Narvaez and Castillo, 2007; Pan et al., 2002) should prevent SR refilling and force recovery. Figure 3 illustrates the tetanic contractions from the initial 0Ca trials (Figures 3A and C) and the 2-APB trials using the two different approaches (Figures 3B and D, see Methods for details) from representative fibers from the Old Affected group. The fiber data in Figure 3A and B illustrate ~50% tetanic force decline in Ca^{2+}-free solution in both trials, and recovery of >95% of baseline force after re-exposure to physiological $[Ca^{2+}]_O$ regardless of the presence of 2-APB in the solution. The fiber data in Figures 3C and D show a more dramatic tetanic force decline in Ca^{2+}-free solution (>96% decline). By the end of the first trial force recovers to ~83% of baseline force, but after a 5 min recovery 95% of force was recovered (data not shown). In the second trial, tetanic force again declines >96% in Ca^{2+}-free solution and recovers 96% of baseline force after re-exposure to physiological $[Ca^{2+}]$ in the presence of 2-APB. Combined data from all experiments indicate an average ~58% force decline in Ca^{2+}-free solution, followed by recovery of ~85% of baseline force in physiological $[Ca^{2+}]$ with 2-APB in solution, regardless of whether 2-APB was introduced in Ca^{2+}-free solution or in conjunction with physiological $[Ca^{2+}]$. An average of ~90% of baseline force was recovered in all fibers by the end of the trial in physiological solution with no 2-APB. After 5-min recovery periods, fibers recovered 100% of baseline force on average.

Examination of triad membrane structures and ryanodine receptor localization

We used electron microscopy to analyze any changes evident in the triad membrane structures in muscles from aged mice in our colony (FVB) and from the NIA colony (DBA). As both FDB and EDL muscles undergo age-related external -Ca^{2+} -dependent EC coupling (Payne et al., 2004a; Payne et al., 2004b) we preferred to switch to the latter for EM and immunostaining experiments due to the more complete ultrastructural characterization in the literature (Klueber and Feczko, 1994). Examination of overall triad/SR arrangement and organization indicates that triads in young muscle are very well-ordered, and their location corresponds with virtually every myofibril at the A–I junction (black arrows, Figures 4A and B). The number of “normal” triads (135) represented 96% of the total number analyzed (140). Triads in aged muscle can also be found to be very well-ordered (black arrows, Figure 4C) or quite disorganized (white arrows, Figure 4D). The number of normal triads (71)

represented 60% of the total number of triads analyzed (121) while the remaining (40%) exhibited longitudinally oriented sarcotubular system. These data in aged mouse muscle are in agreement with that found in aged human muscle (Boncompagni et al., 2006). Overall triad organization does not speak to the possibility of fragmentation of the SR in aged muscle. Closer examination of triad structure reveals that the SR terminal cisternae can appear fragmented in muscle from both young (Figure 4B) and old mice (Figures 4C and D). The fragmented appearance of SR is likely due to the fact that the thin sections were cut through many convolutions or infoldings of the SR network, thus giving the appearance of separate membrane structures. For example, what appear to be fragmented SR terminal cisternae were always in the vicinity of a TT; we could not find large areas of systematically fragmented SR not in the vicinity of a TT. Higher magnification micrographs of triads and SR reveal that the longitudinal SR often appears fragmented in muscle from both young (Figures 5A, B, and C) and old mice (Figures 5E, F, and G). Again, the fragmented appearance of the longitudinal SR is likely due to thin sections exposing convolutions of membranes of the SR network. Accordingly, it was actually quite rare to find examples of triads in which the SR appeared continuous for more than 500nm in fibers from young (4.2 ± 1.3%) (Figure 5D) and old (5.5 ± 1.2%) (Figure 5H) mice. The most systematic alterations evident in triad membrane structures in aged muscle were that of TTs with large profiles (or elongated TTs having large contact surfaces with SR membranes), in agreement with Boncompagni et al. (Boncompagni et al., 2006). Figures 5I and J illustrate these types of TTs adjacent to normal TTs in the same micrograph taken from an aged mouse muscle fiber.

To examine the possibility that EM sections may not reveal segregated pools of releasable Ca^{2+}, we immunostained stretched longitudinal sections from EDL muscles for RyR1 and acquired images on a confocal microscope. Immunofluorescent staining in muscle from both young and old mice reveals the typical double-row staining of triad proteins on either side of the Z-line with a wide gap in the middle of the sarcomere (Figures 6A and D). Analysis of the fluorescence intensity profiles (Figures 6C and F) of double-rows shows that the area in the sarcomere (middle of pictures in Figures 6B and E) displays no more than baseline fluorescence, indicating no RyR1 in this area in the 24 fibers analyzed for young and old mice. These data, combined with the absence of segregated SR away from TTs, suggest that there is no readily releasable pool of SR Ca^{2+} that is segregated from voltage control – i.e., the TT, in aging skeletal muscle.

Role of membrane charge screening in external Ca^{2+}-dependent contraction in aged mouse muscle fibers

While conducting contractile experiments using single intact fibers in Ca^{2+}-free solution, we have observed a phenomenon in some fibers in which force decline is accompanied by changes in the nature of the contraction. That is, some tetanic contractions elicited at 100 Hz become unfused during the period of Ca^{2+}-free solution perfusion; and in some cases, fibers only exhibit twitches instead of tetanic contractions. In most of these cases, the twitch force is actually below the baseline twitch force for the muscle. Figure 7 shows an example of a fiber which exhibited this contractile behavior. The baseline trace shows both a twitch and maximal tetanic contraction superimposed. The next four traces, Tetanic #74-#77, show the responses to 300-ms trains of pulses at 100 Hz while the fiber was perfused with Ca^{2+}-free solution. Each response becomes smaller, showing unfused tetani (#74, #75), a twitch response only (#76), and no response at all (#77). Note that these particular traces exhibit lower force than even the baseline twitch force. To examine this phenomenon further, we conducted experiments to probe the possibility that the absence of external Ca^{2+} reduces action potential firing, leading to force decline. To this end, single intact FDB muscle fibers were dissected from aged mice and subjected to similar experiments utilizing both Ca^{2+}-free and Ca^{2+}-free/high-Mg^{2+} solutions (see Methods).

It has been shown that Mg^{2+} is much less effective at screening negative charges at the membrane than Ca^{2+} (Dorrscheidt-Kafer, 1976, 1979b, 1979a). Therefore, force decline in FDB fibers from aged mice was compared in our standard Ca^{2+}-free solution (Ca^{2+} offset with equimolar Mg^{2+}), and in a Ca^{2+}-free solution in which the [Mg^{2+}] was raised to 5 mM in order to compensate for its lesser charge screening capabilities. Figure 8A shows that the average force decline displayed by single intact FDB fibers in Ca^{2+}-free solution is similar to the force decline in Ca^{2+}-free/high-Mg^{2+} solution. Figure 8B shows force traces (top row) and intracellular fluo-4 fluorescence signals (representative of intracellular Ca^{2+} transients; bottom row) from one fiber at baseline (1, 4), after 10 min in Ca^{2+}-free solution (2, 5), and after 10 min following return to physiological solution (3, 6). Figure 8C shows force and fluorescence traces from the same fiber in response to the same contractile protocol using Ca^{2+}-free/high-Mg^{2+} solution. Force and the intracellular Ca^{2+} transient decline in parallel, and the decline in both force and intracellular Ca^{2+} is similar in both Ca^{2+}-free solution and Ca^{2+}-free/high-Mg^{2+} solution. Paired student's t-test reveals no difference between force decline in either solution (p=0.965), while regression comparing force decline in the two solutions revealed significant correlation between the two conditions (r^2=0.892). There were no fibers which displayed force decline in one solution but not the other.

Repetitive action potential generation

To further examine the role of altered membrane excitability causing dependence on external Ca^{2+} in fibers from old mice, we measured the generation of repetitive action potentials of FDB fibers under two-electrode current clamp in recording conditions similar to those used for muscle contraction. These experiments again distinguished two groups of fibers from old mice, Affected (n = 6 fibers, n = 3 mice) and Unaffected (n = 8 fibers, n = 3 mice) by omitting extracellular Ca^{2+}. The Old Unaffected fibers were similar to the fibers from young mice (n = 8 fibers, n = 3 mice), while the Old Affected exhibited a significant number of action potential failures when exposed to Ca^{2+}-free solution. There were no differences in resting membrane potential among the three groups: young (−75 ± 2.2mV), Old Affected (−76 ± 2.5), and Old Unaffected (−74 ± 2.6mV). The initial resting membrane potential recorded in each fiber was held throughout the experiment by current-clamp.

We stimulated fibers with 50, 75 and 100 Hz trains for 350ms. Figure 9 illustrates the generation of repetitive action potentials in response to 100Hz trains in an Old Affected (A) and an Old Unaffected (B) FDB fiber. The resting membrane potentials for these fibers were −75 and −74mV, respectively. In control solution (1.8mM Ca^{2+}), every action potential exhibits an overshoot in both fibers. In Ca^{2+}-free solution, 34 out of 35 action potentials failed in the Old Affected fiber. In contrast, the Old Unaffected fiber showed 35 action potentials with no failures. The amplitudes of the first and last action potentials were compared within the 10^{th} train of pulses in Ca^{2+}-free solution (Table 1). The action potential amplitude in Old Affected fibers was significantly reduced in Ca^{2+}-free solution compared to standard physiological solution (Figure 9A and Table 1). In contrast, Old Unaffected fibers retain the ability to generate normal action potentials when subjected to the same stimulation regimen in Ca^{2+}-free solution (Figure 9B). The rise and decay phases of the action potential or abortive responses did not differ significantly among control, 0Ca solution, or during recovery in 1.8mM Ca^{2+} in Old Affected fibers (Table 1). This result indicates that no major alteration in sodium and potassium kinetics occurs when the fiber is exposed to Ca^{2+}-free solution.

Discussion

This work supports the conclusion that external Ca^{2+} ions are necessary for the maintenance of intracellular Ca^{2+} release and force generation in a population of muscle fibers from aged mice, and that this age-related dependence on external Ca^{2+} is probably due to a failure of

repetitive action potential generation at high frequency stimulation and consequently EC coupling and not a dependence on influx of Ca^{2+} ions or depletion of internal Ca^{2+} stores.

External Ca^{2+} dependence and Ca^{2+} influx

We previously suggested that force decline in a population of fibers from aged mice in the absence of external Ca^{2+} may be due to the absence of Ca^{2+} influx into the cell, further suggesting that these cells may have undergone some type of switch in the mode of EC coupling which requires influx of external Ca^{2+} to activate Ca^{2+} release from the SR (Payne et al., 2004b). To examine the possibility that the dependence on external Ca^{2+} in old fibers arises from the ablation of Ca^{2+} influx into the cell, we performed experiments in which Cd^{2+} was included in solutions to block DHPR I_{Ca} (Tanabe et al., 1990a; Wang et al., 1999). Fibers which exhibited force decline during repeated contraction in Ca^{2+}-free solution exhibited no force decline in the presence of both Ca^{2+} and Cd^{2+}. These data indicate that the presence of external Ca^{2+} is necessary for proper EC coupling in this population of muscle fibers from aged mice (~50% of fibers in aged mice (Payne et al., 2004b)), but that the influx of Ca^{2+} ions is not necessary. Besides, the timing and flux rate of skeletal muscle DHPR I_{Ca} is probably too slow to be of any consequence in EC coupling. By comparison, action potentials in skeletal muscle last for roughly 5 msec, DHPR activation (charge movement, Q_{on}) occurs in 5–10 msec, SR Ca^{2+} release is elicited directly by Q_{on}, and a twitch in FDB muscle fibers at 20°C reaches its peak in roughly 30 msec ((Berne and Levy, 1998) and data from our laboratory). DHPR I_{Ca} under voltage-clamp conditions does not start until after some charge has moved, and the time to peak current amplitude is roughly 75–100 msec (Delbono, 1992; Payne et al., 2004b). I_{Ca} has also been shown to be so small compared to SR Ca^{2+} release flux that it is considered negligible toward cytoplasmic Ca^{2+} elevations during fiber depolarization (Brum et al., 1988; Brum et al., 1987; Ursu et al., 2005). Therefore, in response to action potentials, it is highly unlikely that I_{Ca} is activated to any degree substantial enough to contribute to EC coupling or the global Ca^{2+} transient. Consequently, it is highly unlikely that the force decline exhibited by muscle fibers from aged mice in Ca^{2+}-free solution is due to the loss of Ca^{2+} influx into the cell upon fiber depolarization.

External Ca^{2+}-dependence and SR Ca^{2+} depletion

In a previous report, we suggested that a possible cause of external Ca^{2+}-dependent contraction in aged mouse muscle fibers was that the SR becomes depleted of Ca^{2+}, thus reducing the amount of released Ca^{2+} and reducing force in Ca^{2+}-free solution (Payne et al., 2004b). It has been shown in skeletal muscle that the SR can be depleted of Ca^{2+} in externally Ca^{2+}-free conditions, and that upon reexposure to external Ca^{2+}-containing solution intracellular stores are rapidly refilled via SOCE (Kurebayashi and Ogawa, 2001). It has also been shown that SOCE is blocked by the drug 2-APB (Prakriya and Lewis, 2001). However, the procedure to deplete the SR is very prolonged and involves high $[K^+]$ contractures and SERCA inhibitors over a time course up to 3 hours. This is probably due to the large amount of SERCA on the SR to immediately uptake cytoplasmic Ca^{2+} (Franzini-Armstrong and Jorgensen, 1994), abundance of calsequestrin to allow a huge Ca^{2+} storage capacity (Ikemoto et al., 1974; MacLennan and Holland, 1975), and the fact that skeletal muscle SR membranes are much less leaky than smooth muscle or non-excitable cells (Murayama et al., 2000; Ogawa et al., 1999). It therefore seemed unlikely that our procedure of tetanic contractions over 10 min in Ca^{2+}-free solution depleted the fibers of Ca^{2+} to the level that force was not detectable in some fibers. Nevertheless, others have shown that rapid contractions in Ca^{2+}-free solution may deplete SR Ca^{2+} in aged muscle fibers (Weisleder et al., 2006). However, our data show that in fibers exhibiting nearly 100% force decline in Ca^{2+}-free solution, all fibers produced robust 4-CmC contractures (~98% of baseline force). These data indicate that the SR contained a large amount of Ca^{2+} available

for release. In the aforementioned work by Kurebayashi and Ogawa, the investigators found that contractures by exposure to high [K^+] in the absence of external Ca^{2+} eventually became undetectable. However, after addition of a SERCA blocker, contractures once again became robust, indicating that prior to SERCA blocker application the SR contained Ca^{2+} (partially depleted), but upon its release the Ca^{2+} was taken up into the SR before it could reach the contractile apparatus (Kurebayashi and Ogawa, 2001). It is possible that our experiments produce this partially depleted state in the SR of Old Affected fibers, and that the 4-CmC is releasing the remaining Ca^{2+}. However, since we did not include a SERCA blocker in our experiments, reuptake of the Ca^{2+} should not be affected and 4-CmC contractures should be very small to non-existent in these fibers. Therefore, these data suggest that force decline in aged fibers in Ca^{2+}-free solution is not due to SR Ca^{2+} depletion.

Other investigators have found that upon force decline in Ca^{2+}-free solution due to SR Ca^{2+} depletion, caffeine contractures are still produced in fibers from aged mice but not young (Weisleder et al., 2006). These authors conclude that a segregated store of voltage-insensitive Ca^{2+} exists in these fibers – similar to MG29 knockout mutants (Kurebayashi et al., 2003) – and may be due to the age-related decline in MG29 expression (Weisleder et al., 2006). It was consequently found in MG29 knockouts that SOCE is activated in fibers even before caffeine contractures were elicited, suggesting the voltage-controlled store of Ca^{2+} was depleted, but the voltage-insensitive store was not (Kurebayashi et al., 2003). Therefore it may be possible that our experiments deplete a voltage-controlled store of Ca^{2+} while the 4-CmC contractures release the segregated store of Ca^{2+} in fibers from aged mice. To examine this, we utilized 2-APB to block potential SOCE upon return to physiological solution in our experiments. We found that 2-APB did not block recovery of tetanic force in muscle fibers from aged mice that displayed force decline in Ca^{2+}-free solution. This lack of effect was seen whether the drug was introduced simultaneously with external Ca^{2+} or 5 min prior to return of external Ca^{2+}. These results suggest that tetanic force decline in our experiments in Ca^{2+}-free solution is not due to depletion of voltage-controlled SR Ca^{2+} store, and further suggest that force recovery in physiological solution is not due to SOCE.

External Ca^{2+} dependence and altered membrane structures

In conjunction with the hypothesis of a segregated Ca^{2+} store in aged muscle fibers, structural changes to the SR network in aged fibers, such as swollen TTs and fragmented SR networks were described (Weisleder et al., 2006). Upon examination of EM micrographs of triads within muscle from young and old mice, we found many examples of what appear to be fragmented SR networks, both in the longitudinal SR and the terminal cisternae, in muscle fibers from both young and old mice. In fact, it was more common to find SR membranes that appeared fragmented than intact luminal structures. We found a higher incidence of overall triad disorganization in fibers from aged mice, similar to the findings of Boncompagni et al. (Boncompagni et al., 2006). Part of the disorganization described in aged muscle is a reduction in triad density in aged human muscle fibers. This provides morphological evidence to support our previous findings of EC uncoupling in aged muscle (Delbono et al., 1995; González et al., 2000; Renganathan et al., 1997; Wang et al., 2000). While disorganization of the triad membrane structures in aging is an intriguing development in EC uncoupling, a potential triad membrane-associated mechanism for external Ca^{2+}-dependent contraction in aged fibers is not obvious in that report or in ours. The supposed fragmented SR terminal cisternae we found in muscle fibers from young and old mice were always in the vicinity of a TT, suggesting that they would be under voltage control. Furthermore, we were unable to find any extensively fragmented SR networks as suggested (Weisleder et al., 2006).

It is possible that the EM micrographs may have missed some type of alternative localization of SR containing RyR1 not linked to DHPR. In order for a segregated, membrane-bound store of Ca^{2+} to be released upon caffeine or 4-CmC exposure, that store must contain RyR1. To examine the organization of RyR1 in aged muscle, we stretched and fixed bundles of muscle fibers from young and old mice for immunostaining. The typical double-row staining in both young and old muscle fibers reveals that the subcellular localization of RyR1 does not change in aged muscle. While the expression of DHPR does decline with age, leading to a reduction in the DHPR-RyR1 ratio (EC uncoupling) (Delbono et al., 1995; Renganathan et al., 1997; Wang et al., 2000), it seems that the RyR1 do indeed stay localized at the triads, where DHPRs are also found. Therefore, while fewer RyR1s are coupled to DHPRs in aged muscle, our data suggest the uncoupled RyR1s do no represent a storage pool of Ca^{2+} segregated from voltage controlled release.

External Ca^{2+}-dependence and sarcolemmal excitability

The tetanic contraction force traces from fibers exhibiting dramatic force decline in Ca^{2+}-free solution often resembled those elicited by lower frequency stimulation; that is, they became unfused tetani similar to those elicited by 50 Hz stimulation. Also, some fibers produced only single twitches in response to trains of pulses at 100 Hz. Our Ca^{2+}-free solution replaced Ca^{2+} with an equimolar concentration of Mg^{2+}, making Mg^{2+} the primary divalent cation in the external solution. It has been shown that Mg^{2+} is only about half as effective at screening negative charges on the outer leaf of the membrane versus Ca^{2+} (Dorrscheidt-Kafer, 1976, 1979b, 1979a). We therefore surmised that the ability of these fibers to fire action potentials might be impaired. However, adding Mg^{2+} to the solution to compensate for its reduced charge screening ability did not change the outcome of the experiments. Fibers showed equal decline in tetanic force and intracellular Ca^{2+} transients in our standard Ca^{2+}-free solution and the Ca^{2+}-free solution with elevated Mg^{2+} (see Methods), suggesting that abnormal membrane charge screening is not the primary cause of force decline in Ca^{2+}-free solution in fibers from aged mice.

As mentioned above, muscle fibers in aging muscle undergo a slow denervation process (Einsiedel and Luff, 1992; Kadhiresan et al., 1996; Larsson and Ansved, 1995; Wang et al., 2005). This process is accompanied by a slow depolarization of the membrane resulting from altered Na^+ and K^+ permeability and leading to inactivation of Na^+ currents (Kotsias and Venosa, 1987, 2001). The slower time course of action potentials leads to missing events during a train of pulses, and, in some fibers, only single action potentials during a train of pulses (Kotsias and Muchnik, 1987). These changes were found in normal Ringer solution, whereas our results were collected in Ca^{2+}-free solutions. Therefore, while potential alterations to Na^+ channels during aging may explain our data, the published findings in denervated muscle do not fully explain our results.

In 43% of the fibers from old mice, approximately 97% of the action potentials failed in response to 100Hz stimulation pulses Ca^{2+}-free solution. This finding correlates with the decline in tetanic force in Old Affected fibers reported here and previously (Payne et al., 2004b). Failing action potentials can lead to decreased intracellular Ca^{2+} release and force during high-frequency stimulation (100Hz).

Nominally Ca^{2+}-free Ringer solution induces amphibian skeletal muscle depolarization (Usher-Smith et al., 2006). However, if this mechanism were responsible for failures in action potential generation, it should affect all FDB fibers from both young and old mice, but the ability to generate action potentials in external Ca^{2+}-free solution was impaired in only 43% of the fibers from old mice and almost no fibers from young mice. This observation supports the concept that the mechanism underlying action potential failures does not depend exclusively on the absence of external Ca^{2+} but also on sodium channel

dysregulation with aging. Muscle denervation and increased TTX-resistant sodium channels have been reported in aging muscle (Wang et al., 2005). However, whether $Na_v1.5$ is more susceptible to external Ca^{2+} omission than the normal skeletal muscle $Na_v1.4$ channel is not known. Altered Na^+ channel properties (namely, conductance) have been shown in roughly half of the fibers from aged rats, which suggests that posttranslational modifications account for some of the differences observed between young and old (Desaphy et al., 1998). For example, the level of sialylation has been shown to play an important role in the voltage dependence of skeletal muscle Na^+ channel gating (Bennett et al., 1997). These researchers also showed that the level of sialylation influenced the channel's sensitivity to external Ca^{2+} (Bennett et al., 1997). Alterations to posttranslational channel modifications, such as various types of glycosylation, in aged muscle fibers could explain our findings when external $[Ca^{2+}]$ is reduced. As another potential mechanism, modification during aging in the lipid bilayer surrounding sodium channels may influence their permeation and gating properties (Ji et al., 1993). Whether the inwardly rectifying potassium channel is altered in a fraction of aging muscle fibers is not known. Although the lack of significant changes in the action potential decay phase indicates that this explanation is unlikely, further studies are needed.

In conclusion, the data reported here indicate that external Ca^{2+} but not Ca^{2+} influx is needed to maintain force during fiber repetitive electrical stimulation in a population of aging fibers. SR Ca^{2+} depletion, SOCE, and the putative segregated Ca^{2+} release store do not play a significant role in external Ca^{2+}-dependent contraction in aging muscle. Failure to generate action potentials in 0Ca solution explains the decreased intracellular Ca^{2+} mobilization and depressed tetanic force in Old Affected fibers.

Acknowledgments

We thank Gregory Piccola for technical assistance on the EM studies. The present study was supported by grants from the National Institutes of Health/National Institute on Aging (AG07157 and AG15820) and the Muscular Dystrophy Association to Osvaldo Delbono, and by the Wake Forest University Claude D. Pepper Older Americans Independence Center (P30-AG21332).

References

Airey JA, Beck CF, Murakami K, Tanksley SJ, Deerinck TJ, Ellisman MH, Sutko JL. Identification and localization of two triad junctional foot protein isoforms in mature avian fast twitch skeletal muscle. J Biol Chem. 1990; 265:14187–14194. [PubMed: 2387846]

Armstrong CM, Bezanilla FM, Horowicz P. Twitches in the presence of ethylene glycol bis(-aminoethyl ether)-N,N'-tetracetic acid. Biochim Biophys Acta. 1972; 267:605–608. [PubMed: 4537984]

Bennett E, Urcan MS, Tinkle SS, Koszowski AG, Levinson SR. Contribution of sialic acid to the voltage dependence of sodium channel gating. A possible electrostatic mechanism. J Gen Physiol. 1997; 109:327–343. [PubMed: 9089440]

Berne, R.; Levy, M. Generation and Conduction of Action Potentials. In: Koeppen, B.; Stanton, B., editors. Physiology. Fourth Edition ed.. St. Louis: Mosby; 1998. p. 30-42.

Boncompagni S, d'Amelio L, Fulle S, Fano G, Protasi F. Progressive disorganization of the excitation-contraction coupling apparatus in aging human skeletal muscle as revealed by electron microscopy: a possible role in the decline of muscle performance. J Gerontol A Biol Sci Med Sci. 2006; 61:995–1008. [PubMed: 17077192]

Bootman MD, Collins TJ, Mackenzie L, Roderick HL, Berridge MJ, Peppiatt CM. 2-aminoethoxydiphenyl borate (2-APB) is a reliable blocker of store-operated Ca2+ entry but an inconsistent inhibitor of InsP3-induced Ca2+ release. Faseb J. 2002; 16:1145–1150. [PubMed: 12153982]

Brum G, Stefani E, Rios E. Simultaneous measurements of Ca2+ currents and intracellular Ca2+ concentrations in single skeletal muscle fibers of the frog. Can J Physiol Pharmacol. 1987; 65:681–685. [PubMed: 2440542]

Brum G, Rios E, Stefani E. Effects of extracellular calcium on calcium movements of excitation-contraction coupling in frog skeletal muscle fibres. J Physiol. 1988; 398:441–473. [PubMed: 2455801]

Delbono O. Calcium current activation and charge movement in denervated mammalian skeletal muscle fibres. J Physiol. 1992; 451:187–203. [PubMed: 1328616]

Delbono O. Neural control of aging skeletal muscle. Aging Cell. 2003; 2:21–29. [PubMed: 12882331]

Delbono O, O'Rourke KS, Ettinger WH. Excitation-calcium release uncoupling in aged single human skeletal muscle fibers. J Membr Biol. 1995; 148:211–222. [PubMed: 8747553]

Desaphy JF, De Luca A, Imbrici P, Conte Camerino D. Modification by ageing of the tetrodotoxin-sensitive sodium channels in rat skeletal muscle fibres. Biochim Biophys Acta. 1998; 1373:37–46. [PubMed: 9733912]

Dorrscheidt-Kafer M. The action of Ca2+, Mg2+ and H+ on the contraction threshold of frog skeletal muscle: Evidence for surface charges controlling electro-mechanical coupling. Pflugers Arch. 1976; 362:33–41. [PubMed: 3761]

Dorrscheidt-Kafer M. The interaction of ruthenium red with surface charges controlling excitation-contraction coupling in frog sartorius. Pflugers Arch. 1979a; 380:181–187. [PubMed: 314624]

Dorrscheidt-Kafer M. Excitation-contraction coupling in frog sartorius and the role of the surface charge due to the carboxyl group of sialic acid. Pflugers Arch. 1979b; 380:171–179. [PubMed: 39290]

Dulhunty AF, Gage PW. Effects of extracellular calcium concentration and dihydropyridines on contraction in mammalian skeletal muscle. J Physiol. 1988; 399:63–80. [PubMed: 2457097]

Einsiedel LJ, Luff AR. Alterations in the contractile properties of motor units within the ageing rat medial gastrocnemius. J Neurol Sci. 1992; 112:170–177. [PubMed: 1469429]

Felder E, Protasi F, Hirsch R, Franzini-Armstrong C, Allen PD. Morphology and molecular composition of sarcoplasmic reticulum surface junctions in the absence of DHPR and RyR in mouse skeletal muscle. Biophys J. 2002; 82:3144–3149. [PubMed: 12023238]

Franzini-Armstrong C, Jorgensen AO. Structure and development of E–C coupling units in skeletal muscle. Annu Rev Physiol. 1994; 56:509–534. [PubMed: 8010750]

González-Serratos H, Valle-Aguilera R, Lathrop DA, Garcia MC. Slow inward calcium currents have no obvious role in muscle excitation-contraction coupling. Nature. 1982; 298:292–294. [PubMed: 6806669]

González E, Messi ML, Delbono O. The specific force of single intact extensor digitorum longus and soleus mouse muscle fibers declines with aging. J Membr Biol. 2000; 178:175–183. [PubMed: 11148759]

González E, Messi ML, Zheng Z, Delbono O. Insulin-like growth factor-1 prevents age-related decrease in specific force and intracellular Ca2+ in single intact muscle fibres from transgenic mice. J Physiol. 2003; 552:833–844. [PubMed: 12937290]

Gonzalez Narvaez AA, Castillo A. Ca2+ store determines gating of store operated calcium entry in mammalian skeletal muscle. J Muscle Res Cell Motil. 2007; 28:105–113. [PubMed: 17616822]

Ikemoto N, Nagy B, Bhatmagar GM, Gergely J. Studies on a metal-binding protein of the sarcoplasmic reticulum. J Biol Chem. 1974; 249:2357–2365. [PubMed: 4856651]

Ji S, Weiss JN, Langer GA. Modulation of voltage-dependent sodium and potassium currents by charged amphiphiles in cardiac ventricular myocytes. Effects via modification of surface potential. J Gen Physiol. 1993; 101:355–375. [PubMed: 8386217]

Kadhiresan VA, Hassett CA, Faulkner JA. Properties of single motor units in medial gastrocnemius muscles of adult and old rats. J Physiol. 1996; 493(Pt 2):543–552. [PubMed: 8782115]

Klueber KM, Feczko JD. Ultrastructural, histochemical, and morphometric analysis of skeletal muscle in a murine model of type I diabetes. Anat Rec. 1994; 239:18–34. [PubMed: 8037375]

Kotsias BA, Venosa RA. Role of sodium and potassium permeabilities in the depolarization of denervated rat muscle fibres. J Physiol. 1987; 392:301–313. [PubMed: 3446781]

Kotsias BA, Muchnik S. Mechanical and electrical properties of denervated rat skeletal muscles. Exp Neurol. 1987; 97:516–528. [PubMed: 3622706]

Kotsias BA, Venosa RA. Sodium influx during action potential in innervated and denervated rat skeletal muscles. Muscle Nerve. 2001; 24:1026–1033. [PubMed: 11439377]

Kurebayashi N, Ogawa Y. Depletion of Ca2+ in the sarcoplasmic reticulum stimulates Ca2+ entry into mouse skeletal muscle fibres. J Physiol. 2001; 533:185–199. [PubMed: 11351027]

Kurebayashi N, Takeshima H, Nishi M, Murayama T, Suzuki E, Ogawa Y. Changes in Ca2+ handling in adult MG29-deficient skeletal muscle. Biochem Biophys Res Commun. 2003; 310:1266–1272. [PubMed: 14559251]

Lannergren J, Westerblad H. The temperature dependence of isometric contractions of single, intact fibres dissected from a mouse foot muscle. J Physiol. 1987; 390:285–293. [PubMed: 3443937]

Larsson L, Ansved T. Effects of ageing on the motor unit. Prog Neurobiol. 1995; 45:397–458. [PubMed: 7617890]

MacLennan DH, Holland PC. Calcium transport in sarcoplasmic reticulum. Annu Rev Biophys Bioeng. 1975; 4:377–404. [PubMed: 125558]

Miller RA, Bookstein F, Van der Meulen J, Engle S, Kim J, Mullins L, Faulkner J. Candidate biomarkers of aging: age-sensitive indices of immune and muscle function covary in genetically heterogeneous mice. J Gerontol A Biol Sci Med Sci. 1997; 52:B39–B47. [PubMed: 9008656]

Murayama T, Kurebayashi N, Ogawa Y. Role of Mg^{2+} in Ca^{2+}-induced Ca^{2+} release through ryanodine receptors of frog skeletal muscle: modulations by adenine nucleotides and caffeine. Biophys J. 2000; 78:1810–1824. [PubMed: 10733962]

Ogawa Y, Murayama T, Kurebayashi N. Ryanodine receptor isoforms in excitation-contraction coupling. Adv Biophys. 1999; 36:27–64. [PubMed: 10463072]

Pan Z, Yang D, Nagaraj RY, Nosek TA, Nishi M, Takeshima H, Cheng H, Ma J. Dysfunction of store-operated calcium channel in muscle cells lacking mg29. Nat Cell Biol. 2002; 4:379–383. [PubMed: 11988740]

Payne AM, Delbono O. Neurogenesis of excitation-contraction uncoupling in aging skeletal muscle. Exerc Sport Sci Rev. 2004; 32:36–40. [PubMed: 14748548]

Payne AM, Messi ML, Zheng Z, Delbono O. Motor neuron targeting of IGF-1 attenuates age-related external Ca(2+)-dependent skeletal muscle contraction in senescent mice. Exp Gerontol. 2007; 42:309–319. [PubMed: 17174053]

Payne, AM.; González, E.; Zheng, Z.; Wang, Z-M.; Messi, ML.; Delbono, O. Cardiac-Like Excitation-Contraction (EC) Coupling in Aging Skeletal Muscle; Annual Meeting of the Society for Experimental Biology; Washington, DC. 2004a.

Payne AM, Zheng Z, Gonzalez E, Wang ZM, Messi ML, Delbono O. External Ca(2+)-dependent excitation--contraction coupling in a population of ageing mouse skeletal muscle fibres. J Physiol. 2004b; 560:137–155. [PubMed: 15297570]

Payne AM, Zheng Z, Messi ML, Milligan CE, Gonzalez E, Delbono O. Motor neurone targeting of IGF-1 prevents specific force decline in ageing mouse muscle. J Physiol. 2006; 570:283–294. [PubMed: 16293644]

Prakriya M, Lewis RS. Potentiation and inhibition of Ca^{2+} release-activated Ca^{2+} channels by 2-aminoethyldiphenyl borate (2-APB) occurs independently of IP(3) receptors. J Physiol. 2001; 536:3–19. [PubMed: 11579153]

Renganathan M, Messi ML, Delbono O. Dihydropyridine receptor-ryanodine receptor uncoupling in aged skeletal muscle. J Membr Biol. 1997; 157:247–253. [PubMed: 9178612]

Renganathan M, Messi ML, Delbono O. Overexpression of IGF-1 exclusively in skeletal muscle prevents age-related decline in the number of dihydropyridine receptors. J Biol Chem. 1998; 273:28845–28851. [PubMed: 9786885]

Rios E, Brum G. Involvement of dihydropyridine receptors in excitation-contraction coupling in skeletal muscle. Nature. 1987; 325:717–720. [PubMed: 2434854]

Saito A, Seiler S, Chu A, Fleischer S. Preparation and morphology of sarcoplasmic reticulum terminal cisternae from rabbit skeletal muscle. J Cell Biol. 1984; 99:875–885. [PubMed: 6147356]

Takagi I, Yamada K, Sato T, Hanaichi T, Iwamoto T, Jin L. Penetration and stainability of modified Sato's lead staining solution. J Electron Microsc (Tokyo). 1990; 39:67–68. [PubMed: 1694216]

Tanabe T, Mikami A, Numa S, Beam KG. Cardiac-type excitation-contraction coupling in dysgenic skeletal muscle injected with cardiac dihydropyridine receptor cDNA. Nature. 1990a; 344:451–453. [PubMed: 2157159]

Tanabe T, Beam KG, Adams BA, Niidome T, Numa S. Regions of the skeletal muscle dihydropyridine receptor critical for excitation-contraction coupling. Nature. 1990b; 346:567–569. [PubMed: 2165570]

Ursu D, Schuhmeier RP, Melzer W. Voltage-controlled Ca2+ release and entry flux in isolated adult muscle fibres of the mouse. J Physiol. 2005; 562:347–365. [PubMed: 15528246]

Usher-Smith JA, Xu W, Fraser JA, Huang CL. Alterations in calcium homeostasis reduce membrane excitability in amphibian skeletal muscle. Pflugers Arch. 2006; 453:211–221. [PubMed: 16955310]

Wang ZM, Messi ML, Delbono O. Patch-clamp recording of charge movement, Ca(2+) current, and Ca(2+) transients in adult skeletal muscle fibers. Biophys J. 1999; 77:2709–2716. [PubMed: 10545370]

Wang ZM, Messi ML, Delbono O. L-Type Ca(2+) channel charge movement and intracellular Ca(2+) in skeletal muscle fibers from aging mice. Biophys J. 2000; 78:1947–1954. [PubMed: 10733973]

Wang ZM, Zheng Z, Messi ML, Delbono O. Extension and magnitude of denervation in skeletal muscle from ageing mice. J Physiol. 2005; 565:757–764. [PubMed: 15890702]

Weisleder N, Brotto M, Komazaki S, Pan Z, Zhao X, Nosek T, Parness J, Takeshima H, Ma J. Muscle aging is associated with compromised Ca2+ spark signaling and segregated intracellular Ca2+ release. J Cell Biol. 2006; 174:639–645. [PubMed: 16943181]

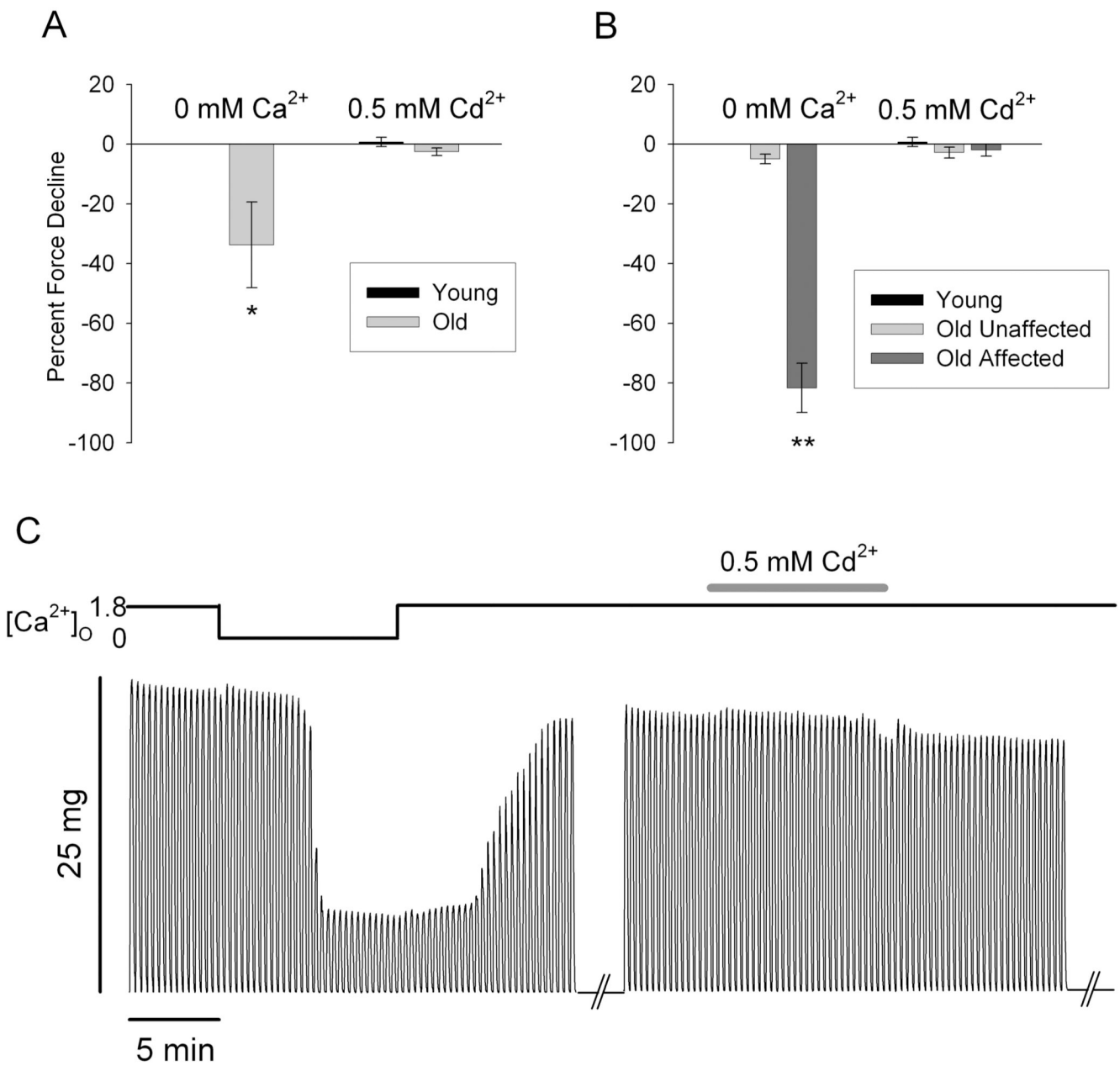

Figure 1. Blocking inward Ca^{2+} current with Cd^{2+} does not cause force decline in muscle fibers from aged mice

A. Force decline in fibers from aged mice is significantly greater in Ca^{2+}-free solution (left) than in solution with 0.5mM Cd^{2+} (right) (*, $p<0.01$; n = 5 fibers from 3 young mice). Force decline in Cd^{2+}-containing solution was not significant. **B**. Fibers from aged mice fall into two categories: Old Unaffected fibers (n = 5 fibers from 3 mice) and Old Affected fibers (n = 7 fibers from 5 mice). Again, the 0Ca solution induced a significant decrease in force (left), while no fibers displayed significant force decline in Cd^{2+}-containing solution (right) (**, $p<0.001$; n = 10 fibers). **C.** Tetanic contraction force in a single intact FDB fiber of an aged mouse from the Affected group exposed to physiological (1.8mM Ca^{2+}), 0Ca^{2+} and 1.8mM Ca^{2+} plus 0.5 mM Cd^{2+} solutions, sequentially (see top bar).

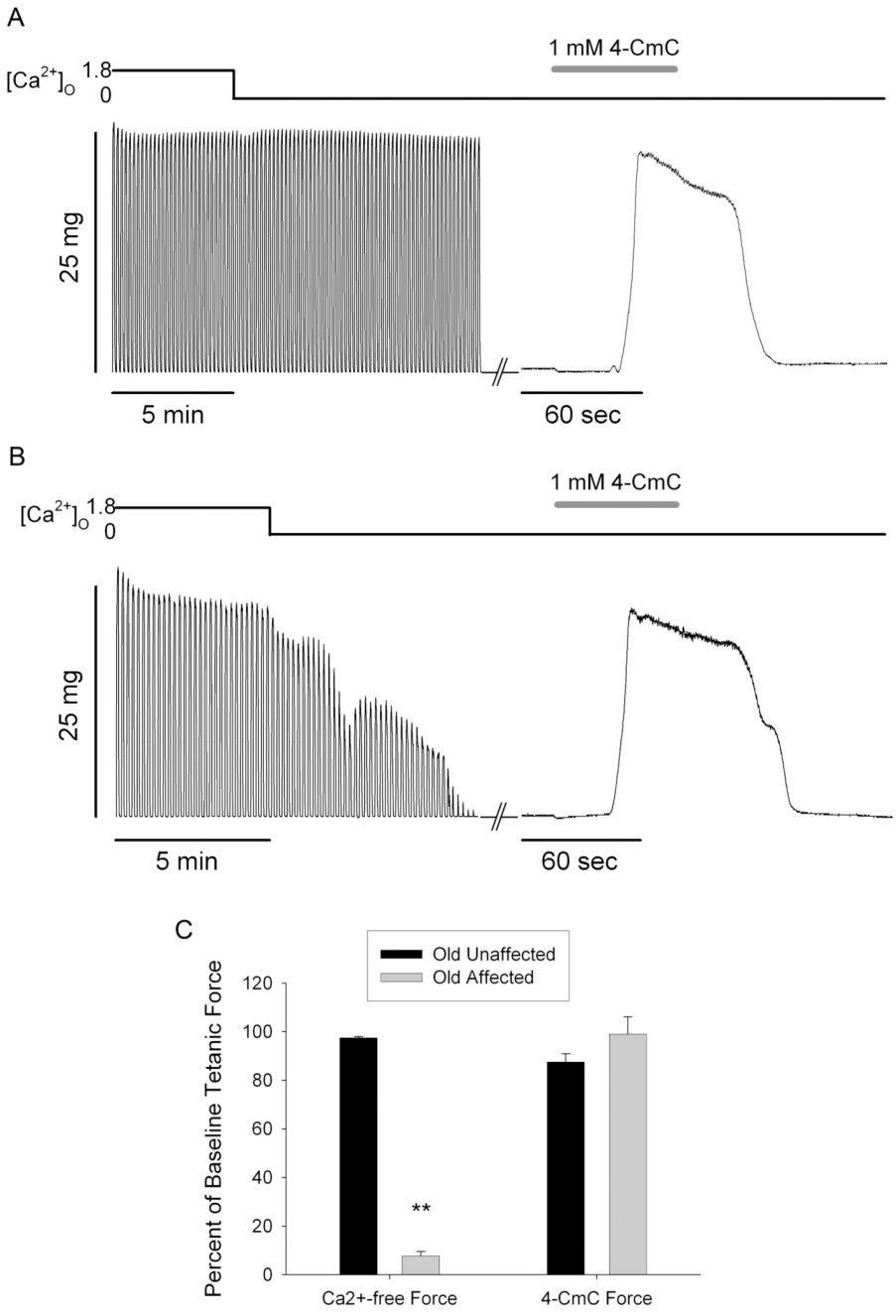

Figure 2. 4-chloro-m-cresol (4-CmC) contractures following repeated tetanic contractions in Ca^{2+}-free solution

A. Sequence of tetanic contractions from a single intact Old Unaffected FDB fiber of an aged mouse in physiological solution, Ca^{2+}-free solution, and 1mM 4-CmC in Ca^{2+}-free solution (see top bar). **B**. Tetanic contractions from a single intact Old Affected FDB fiber in physiological solution, Ca^{2+}-free solution, and 1mM 4-CmC in Ca^{2+}-free solution (see top bar). **C**. Normalized tetanic force at the end of Ca^{2+}-free solution perfusion was significantly decreased in Old Affected fibers compared to Old Unaffected, and was significantly less than the 4-CmC contracture force at the end of the experiment (**, $p<0.001$; n = 4 old unaffected and 6 affected from 3 and 5 mice, respectively). Tetanic force in the Old

Unaffected group was not different from 4-CmC contracture force. 4-CmC contracture force was not different between groups.

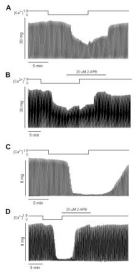

Figure 3. 2-APB action on tetanic force recovery

A and B. Tetani from a single intact FDB fiber of an aged mouse recorded during two exposures to Ca^{2+}-free solution. The traces in A illustrate a 0Ca trial (see Methods). The traces in B illustrate a 2-APB trial in which the 2-APB was introduced during 5 min of contraction in Ca^{2+}-free solution prior to return to normal physiological solution (see Methods). Force decline was virtually identical in the two trials. Note that force recovery in the 2-APB trial occurred in the presence of 1.8 mM Ca^{2+} (physiological solution) and in the presence of 2-APB. **C and D**. Tetani from a single intact FDB fiber of an aged mouse recorded during two exposures to Ca^{2+}-free solution. Traces in C illustrate a 0Ca trial (see Methods). Force decline in this experiment was greater than that illustrated in A and B. Force fully recovered to baseline within 5 min after the experiment (data not shown). Traces in D illustrate a 2-APB trial in which the 2-APB was introduced simultaneously with return to physiological solution. Force fully recovered in the presence of 2-APB. Note the variable onset of the decline in tetanus amplitude after incubating the muscle fiber in Ca^{2+} free medium. Traces are representative of 6 fibers from 6 mice.

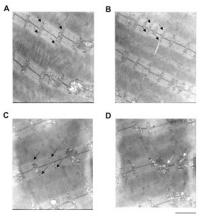

Figure 4. Electron microscopy examination of triad organization

A and B. Samples from young mice taken at 25,000× magnification. Black arrows indicate well-organized triads. **C and D**. Samples from old mice taken at 25,000× magnification. Black arrows indicated well-organized triads in C. White arrows indicate disorganized triad structures in D. Images are representative of 10 fibers from 5 mice. Calibration bar = 1μm.

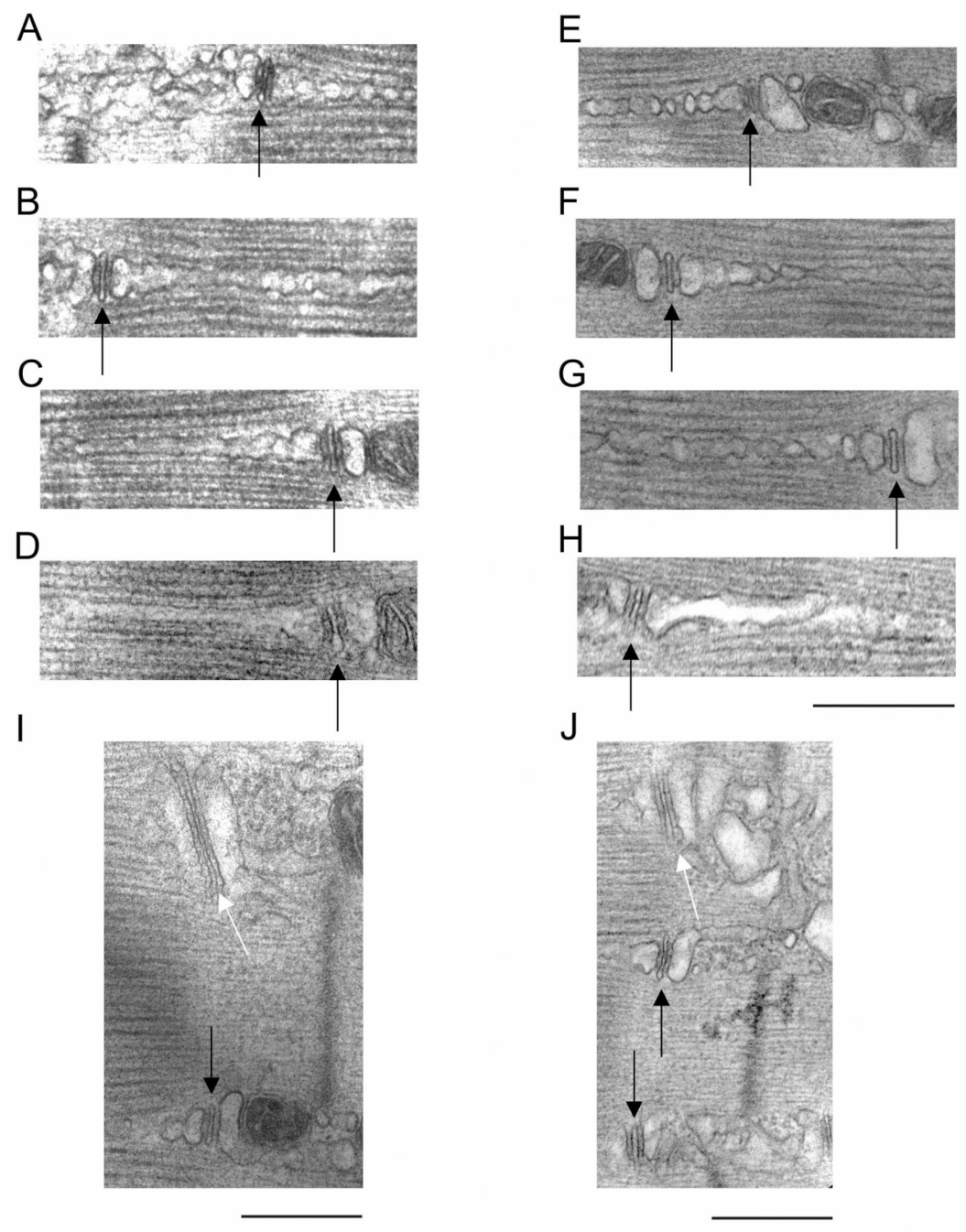

Figure 5. Electron microscopy examination of triad membrane structures

A–D, I. Examples of triads in muscle fibers from young mice taken at 50,000× magnification. Black arrows indicate t-tubules (TT). Note fragmented appearance of longitudinal SR in A–C, and continuous appearance of longitudinal SR in D. Black arrow in **I** indicates a normal TT, while white arrow indicates a rare elongated TT. **E–H, J**. Examples of triads in muscle fibers from old mice taken at 50,000× magnification. Black arrows indicate TTs. Note fragmented appearance of longitudinal SR in **E–G**, and continuous appearance of longitudinal SR in G. Black arrows in J indicate normal TTs, while white arrows indicate elongated TTs. Elongated TTs were more common in muscle fibers from aged mice. (Diagonally cut corners on J occurred from cropping circumstances). Images are

representative of 12 fibers from young and 15 fibers from old mice. Calibration bar for A to H = 1μm. Calibration bar for I and J = 500nm.

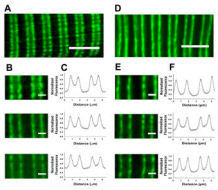

Figure 6. Immunofluorescent staining of RyR1 in stretched muscle fibers from young and old mice

A and D. Examples of immunostaining in muscle fibers from young (A) and old (D) mice. Note the double-row staining pattern for RyR1. Bars = 5μm. **B and E**. Higher magnification (using ImageJ software) images of sarcomeres – Z-lines in the centers of stained double-rows – used for fluorescence intensity profiling seen in **C and F**. Bars = 1μm. All examples from both young and old show double-row staining pattern surrounding Z-lines with baseline fluorescence in the center of the sarcomere. Image analysis was performed on 24 fibers for young and 24 fibers for old mice.

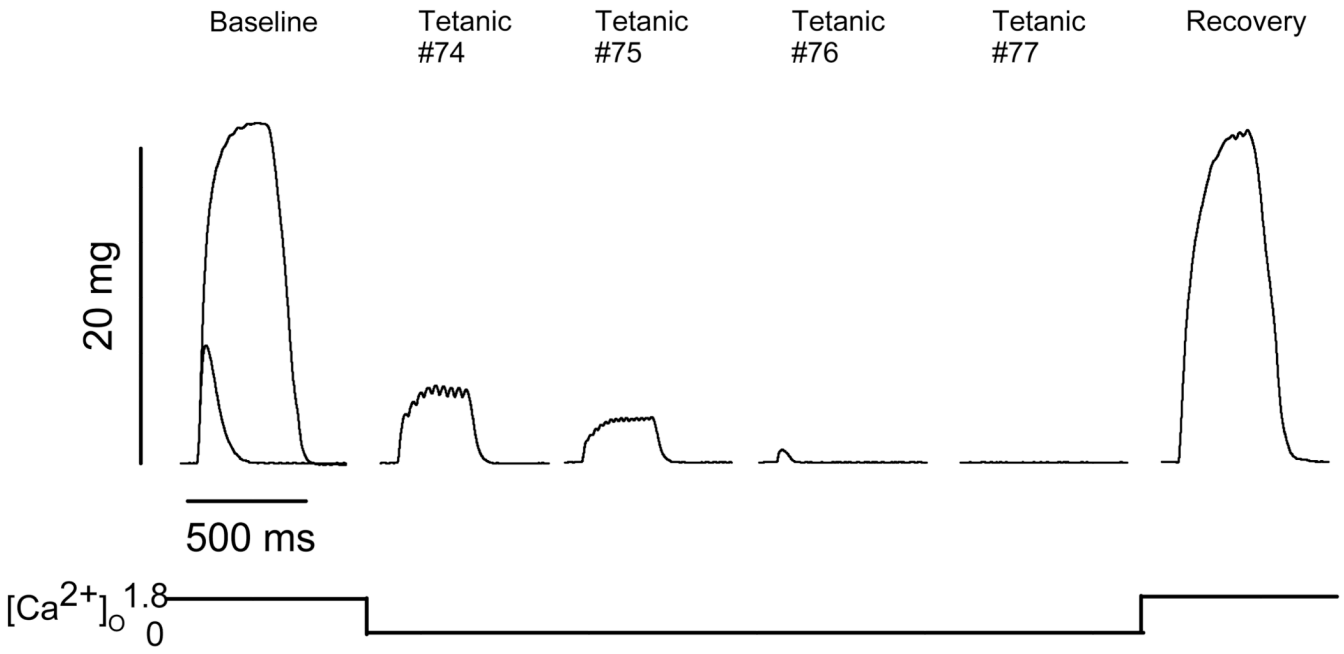

Figure 7. Tetani and twitches recorded in a single intact FDB muscle fiber from an aged (20 mo) FVB mouse

Baseline represents a tetanic trace elicited with a 300-ms train of pulses at 100 Hz superimposed over a single twitch response in physiological solution. Tetanic #74-Tetanic #77 represent responses to 300-ms trains of pulses at 100 Hz while in Ca^{2+}-free solution. The Recovery trace is a tetanic response to a 300-ms train of pulses at 100 Hz in physiological solution 10 min after the end of the experiment. These traces are representative of 10 fibers from 8 mice.

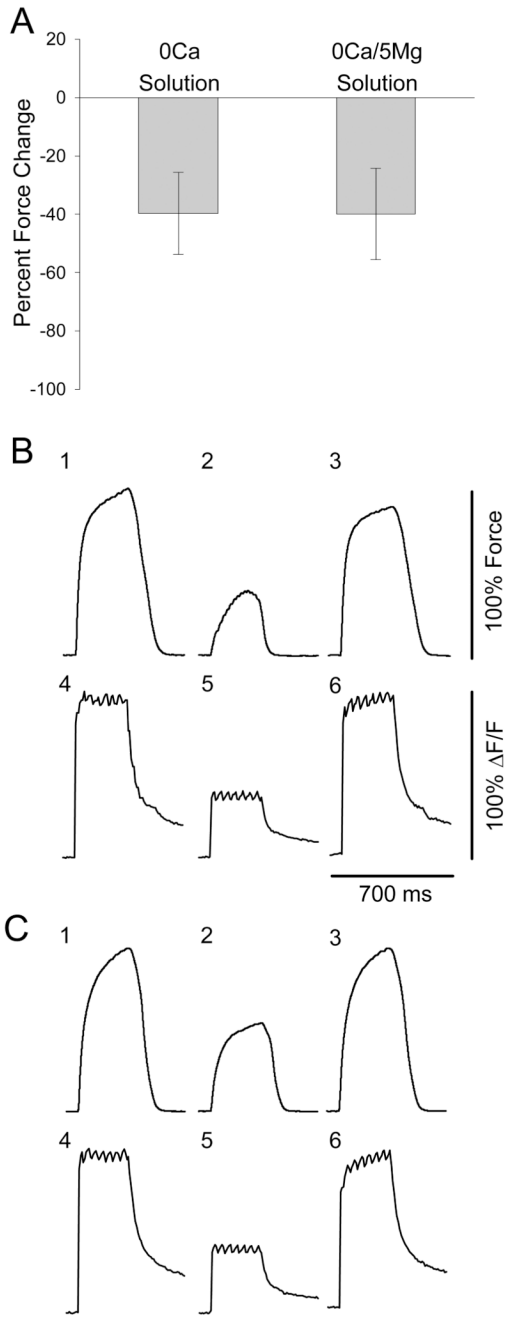

Figure 8. Force decline and intracellular Ca^{2+} transients in Ca^{2+}-free solution and Ca^{2+}-free/ high-Mg^{2+} solution are similar

A. Muscle fibers from aged mice displayed nearly identical average force decline in both Ca^{2+}-free solutions. Paired t-test, p=0.965 (n = 5 fibers from 4 mice). **B and C**. Tetanic contractions (1, 2, 3) and intracellular Fluo-4 fluorescence readings (4, 5, 6) from a single intact FDB fiber of an aged mouse measured simultaneously. One and 4 represent traces from the beginning of the experiment. Two and 5 represent traces after 10 min exposure to either Ca^{2+}-free physiological solution (B) or Ca^{2+}-free/high-Mg^{2+} solution (C). Three and 6 represent traces after 10 min re-exposure to physiological solution.

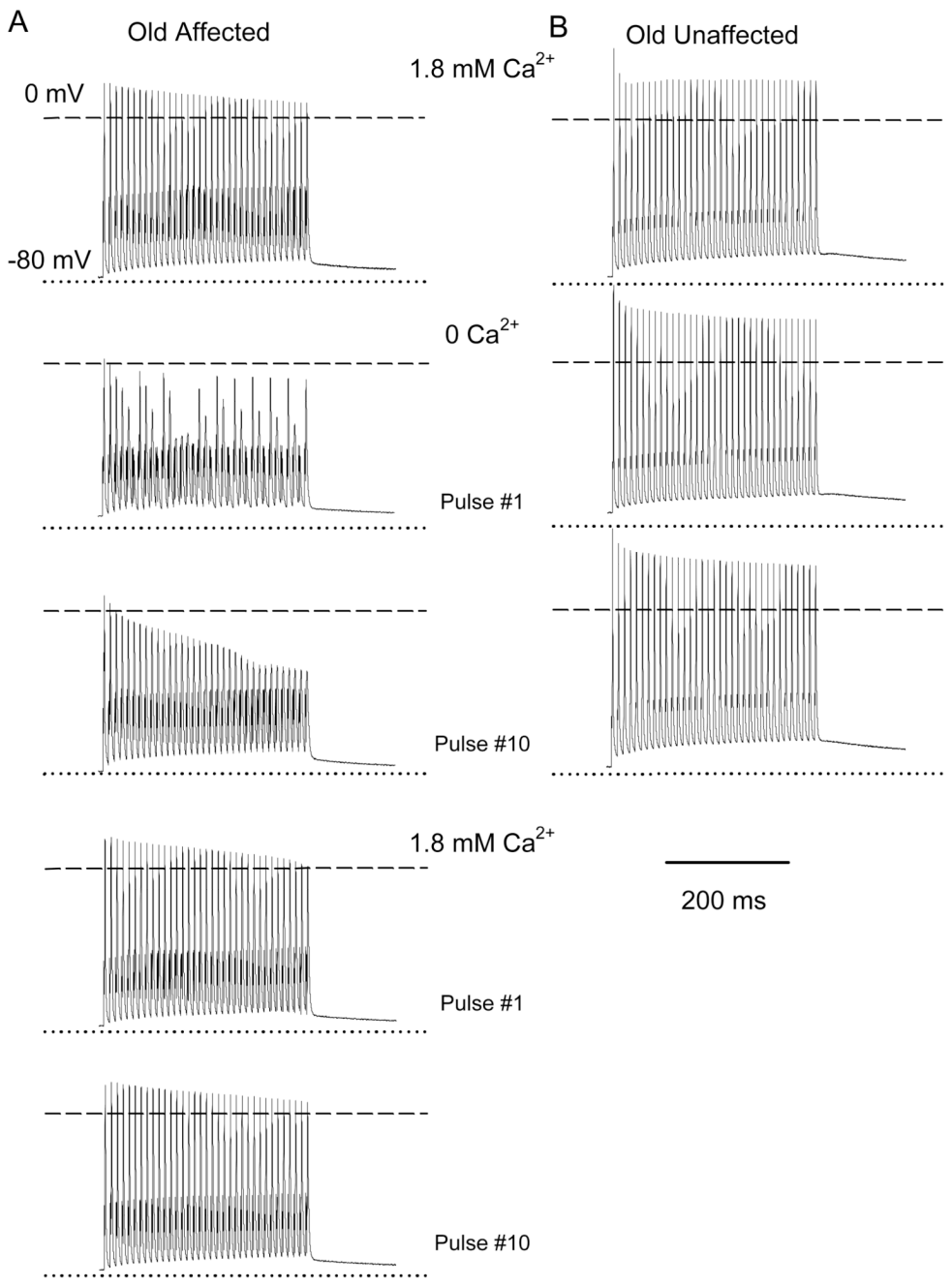

Figure 9. Action potentials in FDB fibers from young and old mice

A and B illustrate trains of action potentials recorded in an Old Affected and Old Unaffected fiber, respectively in response to fiber stimulation at 100 Hz for 350 ms. Recordings in 1.8mM Ca^{2+} (control) and the first and tenth pulses in $0Ca^{2+}$ are shown. The first and tenth pulses in the recovery phase in 1.8mM Ca^{2+} for the old affected fiber are also shown. Dotted and dashed lines indicate the membrane voltage at rest and 0mV, respectively.

Table 1

	Control (1.8mM)	**Test (0 Ca^{2+})**	**Recovery (1.8mM Ca^{2+})**
Action potential rise phase, τ_a (ms)	0.13 ± 0.07	0.14 ± 0.06	0.09 ± 0.08
Action potential decay phase, τ_d (ms)	0.52 ± 0.04	0.56 ± 0.05	0.46 ± 0.03
Last/first action potential amplitude	0.89 ± 0.03	0.63 ± 0.02 (*)	0.92 ± 0.01 ($^{\#}$)
Percent of action potential failures at pulse 10^{th} (%)	0.05 ± 0.02	97.2 ± 1.3 (*)	0.04 ± 0.06 ($^{\#}$)
N fibers	12	6	8

$^{(*)}$ $p < 0.01$, comparing control and test recordings

$^{(\#)}$ $p < 0.01$, comparing test and recovery recordings

τ_a and τ_d were not statistically different among control, test and recovery phases of the experiment.